Novel Expression Pattern of Cytosolic Gln Synthetase in Nitrogen-Fixing Root Nodules of the Actinorhizal Host, *Datisca glomerata*[1[w]]

Alison M. Berry*, Terence M. Murphy, Patricia A. Okubara, Karin R. Jacobsen, Susan M. Swensen, and Katharina Pawlowski

Department of Environmental Horticulture (A.M.B., P.A.O.), and Section of Plant Biology (T.M.M.), University of California, Davis, California 95616; USDA-ARS, Department of Plant Pathology, Washington State University, Pullman, Washington 99164–6430 (P.A.O.); Department of Botany, University of Wisconsin, Madison, Wisconsin 53706 (K.R.J.); Biology Department, Ithaca College, Ithaca, New York 14850 (S.M.S.); Department of Molecular Biology, Agricultural University Wageningen, 6703 HA Wageningen, The Netherlands (K.P.); and Albrecht von Haller Institute for Plant Sciences, Plant Biochemistry, 37077 Göttingen, Germany (K.P.)

Gln synthetase (GS) is the key enzyme of primary ammonia assimilation in nitrogen-fixing root nodules of legumes and actinorhizal (Frankia-nodulated) plants. In root nodules of *Datisca glomerata* (Datiscaceae), transcripts hybridizing to a conserved coding region of the abundant nodule isoform, *DgGS1-1*, are abundant in uninfected nodule cortical tissue, but expression was not detectable in the infected zone or in the nodule meristem. Similarly, the GS holoprotein is immunolocalized exclusively to the uninfected nodule tissue. Phylogenetic analysis of the full-length cDNA of *DgGS1-1* indicates affinities with cytosolic GS genes from legumes, the actinorhizal species *Alnus glutinosa*, and nonnodulating species, *Vitis vinifera* and *Hevea brasilensis*. The *D. glomerata* nodule GS expression pattern is a new variant among reported root nodule symbioses and may reflect an unusual nitrogen transfer pathway from the Frankia nodule microsymbiont to the plant infected tissue, coupled to a distinctive nitrogen cycle in the uninfected cortical tissue. Arg, Gln, and Glu are the major amino acids present in *D. glomerata* nodules, but Arg was not detected at high levels in leaves or roots. Arg as a major nodule nitrogen storage form is not found in other root nodule types except in the phylogenetically related Coriaria. Catabolism of Arg through the urea cycle could generate free ammonium in the uninfected tissue where GS is expressed.

Root nodules are plant organs that are specialized for assimilation of the nitrogen derived from nitrogen fixation by symbiotic bacteria. Cytosolic Gln synthetase (GS1; EC 6.3.1.2) is the key enzyme in primary ammonia assimilation in root nodules of legumes and actinorhizal (Frankia-nodulated) plants (Forde et al., 1989; Guan et al., 1996; Baker and Parsons, 1997). Plant GS is typically expressed at high levels in the infected tissue of root nodules, where in most cases the substrate for the enzyme, ammonium, is released directly from the nitrogen-fixing microsymbiont (O'Gara and Shanmugam, 1976). In the actinorhizal plant *Alnus glutinosa*, GS gene expression is coincident with *nif* gene expression in Frankia-infected nodule cells (Guan et al., 1996), and GS protein is localized in mature infected tissue (Hirel et al., 1982). In many legumes, nodule GS regulation includes additional tissue-specific and developmental components (Padilla et al., 1987; Carvalho et al., 2000; Morey et al., 2002).

Datisca glomerata is an actinorhizal species in the Datiscaceae, a plant family which together with the Coriariaceae forms one of four phylogenetically separate actinorhizal subclades, within the larger angiosperm nitrogen-fixing clade that encompasses legumes and actinorhizal plant taxa (Swensen, 1996; Soltis et al., 2000). Nodulating species in the Datiscaceae and Coriariaceae share a highly distinctive nodule tissue and cellular organization (Hafeez et al., 1984; Silvester et al., 1999; Jacobsen and Berry, 2002) and a distinctive nodule physiology (Tjepkema et al., 1988). As part of an effort to learn more about the evolution of diversity among actinorhizal root nodule symbioses, we have examined expression patterns of several genes in *D. glomerata* nodules (Okubara et al., 1999, 2000; Pawlowski et al., 2003). Here we report a novel pattern of GS gene expression and protein localization in *D. glomerata* root nodules and explore possible metabolic explanations for the spatial patterns observed.

[1] This work was supported by the California Agricultural Experiment Station Project (grant no. 6258–H to A.M.B.), by a Katherine Esau Fellowship, University of California, Davis (to K.P.), and by the NSF (grant no. DEB–9815816 to S.M.S.).

* Corresponding author; e-mail amberry@ucdavis.edu; fax 530–752–1819.

[w] The online version of this article contains Web-only data.

Article, publication date, and citation information can be found at www.plantphysiol.org/cgi/doi/10.1104/pp.103.031534.

RESULTS

GS Genes Expressed in Datisca Root Nodules

Two cDNAs with sequence homology to plant cytosolic GS were cloned from *D. glomerata* root nodules. The first, designated *DgGS1-1*, was isolated from a Datisca nodule cDNA library and is 1,445 nucleotides in length, encoding a deduced polypeptide of 356 amino acids, with a predicted molecular mass of 39 kD. This polypeptide and molecular mass correspond to the range of predicted structures for cytosolic GS subunits in other plant taxa (Forde and Cullimore, 1989). Thirty-two positive cDNA clones in over 160,000 screened hybridized strongly to the *DgGS1-COD* probe. Of these positive clones, four were sequenced and all were derived from *DgGS1-1*. A second isoform, *DgGS1-2*, was obtained by PCR of cDNA made from an enriched pool of Frankia-infected nodule tissue mRNA, using degenerate primers. *DgGS1-2* was 882 bp in length and showed 79% nucleotide sequence identity and 92% amino acid sequence identity to the corresponding portion of *DgGS1-1*. No homologs were found that hybridized to *DgGS1-2*, except one weakly hybridizing clone that was found to be *DgGS1-1*, thus indicating the low abundance of *DgGS1-2* in the nodule cDNA library.

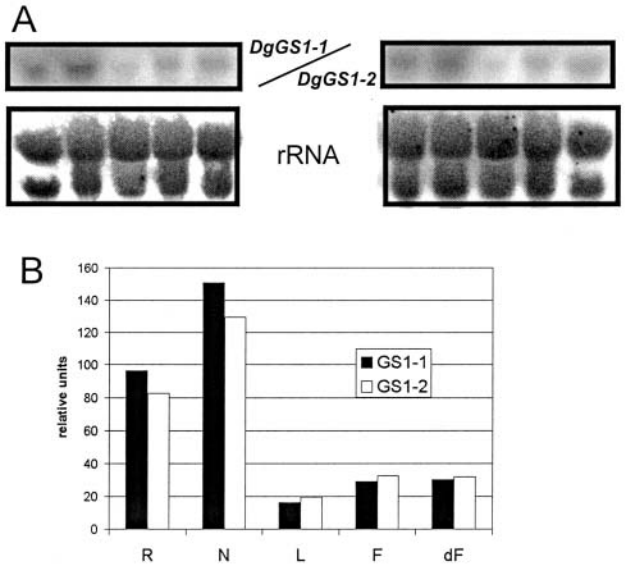

Figure 1. A, DgGS expression levels in different organs of *D. glomerata*. Total RNA from organs of *D. glomerata* (L = leaf, F = flower, dF = developing fruit, R = root, N = nodules; 6 weeks after Frankia inoculation) was hybridized with a gene-specific probe of *DgGS1-1* (left) or with *DgGS1-2* (right). Hybridization of the organ blots with an rRNA probe is shown in the lower sections. B, Image intensity values of GS1-1 and GS1-2 hybridizations relative to rRNA hybridization.

DgGS1-1 Is Expressed in Nodules and Roots

To examine the relative abundance of *DgGS1-1* transcripts in various organs of *D. glomerata*, gel blots of total RNA were hybridized to probes representing the conserved coding region of the full-length *DgGS1-1* cDNA (*DgGS1-COD*) and the partial cDNA of *DgGS1-2*. RNA from all organs hybridized to the probe (Fig. 1A). Expression levels were higher in the root and nodules compared to leaves, flowers, and developing fruits. *DgGS1-2* hybridization was comparable to that of the *DgGS1-COD* probe in nodules and roots relative to other organs (Fig. 1B), probably indicating cross-hybridization with the conserved coding region. Hybridization of organ RNA blots with the *DgGS1-1* 3′-untranslated region (UTR) probe gave results similar to that of *DgGS1-2* (data not shown; *DgGS1-COD* was not compared).

Phylogeny of Datisca Nodule GS

A 1,071-bp portion of the *D. glomerata* nodule GS DNA sequence from clone *DgGS1-1* was included in a phylogenetic analysis of published plant GS sequences, including DNA sequences encoding both cytosolic and plastidic isoforms (Fig. 2). The analysis included the same stretch of the amino acids in the coding region of the GS cDNA sequences and did not include any 3′ or 5′ UTR. The plastidic sequences were designated as the outgroup based on our own previous analyses and that of others (Doyle, 1991; Kumada et al., 1993; Biesiadka and Legocki, 1997). This analysis resulted in a single most parsimonious tree (Fig. 2) of 4,652 steps and a consistency index (Kluge and Farris, 1969) of 0.2604 (excluding autapomorphies). In this tree, *DgGS1-1* clearly groups among the cytosolic GS sequences, not the plastidic GS. *D. glomerata* GS1-1 is sister to GS from *Hevea brasilensis* and both are sister to nodule-expressed GS from *A. glutinosa*. The placement of *DgGS1-1* within this assemblage is moderately well supported with a decay value of three. This phylogenetic analysis also includes legume nodule GS sequences that group according to α, β, and γ subclasses identified previously (Gebhardt et al., 1986; Tingey et al., 1987; Morey et al., 2002). Based on this analysis, the legume β and γ subclasses appear to be most closely related to each other, and *DgGS1-1* is most closely associated with the α subclass of legume GS sequences. The second Datisca sequence (*DgGS1-2*) appears as sister to the α legume clade, but its position has less support than the placement of *DgGS1-1* (decay value of 2).

In an attempt to identify ortholog groups for GS sequences (and thus possibly assign Datisca sequences to an ortholog group), several Arabidopsis sequences were included in this analysis. All of the Arabidopsis GS sequences appeared as part of a large Brassicaceae clade that included *Raphanus sativus* and *Brassica napus*. It appears that Arabidopsis paralogs are confined to the Brassicaceae clade, having duplicated during the divergence of these species. Therefore, at present, Datisca GS appears to have greatest affinity to the α subclass of legume GS; however, the phylogeny does not yet provide a complete picture of angiosperm

GS phylogeny. The sampling of GS1 sequences available for this analysis is relatively sparse, representing only a few of the angiosperm species known to be related to Datisca. Once additional GS sequences become available, the current picture of GS phylogeny will likely be modified.

GS Transcripts Are Expressed Primarily in Uninfected Nodule Tissue

The area of Frankia-infected tissue in nodules of *D. glomerata* can be divided into the zone of infection (zone II in Fig. 3A), where Frankia hyphae proliferate to fill the plant cells; the zone of nitrogen fixation (zone III in Fig. 3, A and F), where Frankia vesicles have differentiated and nitrogen fixation takes place; and the zone of senescence (zone IV in Fig. 3F), where Frankia material is degraded by the plant, according to terminology established by Ribeiro et al. (1995). Frankia-infected tissue was distinguishable in polarizing optics from surrounding uninfected cortical tissue by the absence of birefringence associated with secondary cell walls or starch grains (Fig. 3B). The walls of Frankia-infected host cells in *D. glomerata* are pectin-rich (Jacobsen and Berry, 2002), and amyloplasts do not differentiate in zones II or III.

nifH, encoding a subunit of the nitrogenase enzyme system (Rubio and Ludden, 2002), served as a marker to delineate the nitrogen-fixing zone III in the Frankia-infected nodule tissue sector (Fig. 3, A and B). *nifH* was expressed at highest levels in a zone of infected cells at the earliest stage of nitrogen fixation and at lower levels in the rest of the fixation zone. No *nifH* expression was observed in the infection zone, where Frankia hyphae proliferate in the cortical cells but where vesicles have not differentiated. *nifH* expression was not observed in the zone of senescence, where Frankia material is degraded by the plant.

The GS partial coding region (*DgGS1-COD*) antisense probe hybridized strongly to the Datisca nodule tissue. However the pattern of hybridization was unusual for nodule GS; high levels of transcript were detected in all the cells of the uninfected cortical tissue flanking the infection zone (Fig. 3C). The pattern of in situ hybridization with the 3′ UTR of the *DgGS1-1* full-length cDNA (*DgGS1-UTR*) was essentially the same as that observed for *DgGS1-COD* (Fig. 3D). Within the infected tissue, however, no hybridization could be detected with either the *DgGS1-COD* or the *DgGS1-UTR* probe, except in some nodules where a low level of hybridization could be seen associated with cells where *nifH* was first expressed (Fig. 3E). GS expression above background could not be detected in the nodule vascular tissues (Fig. 3, C and D). No tissue hybridization was detected using the *DgGS1-COD* sense probe (data not shown).

In older nodules, a zone of apparent senescence of infected cells could be observed at the base of the infected zone (Fig. 3F). *DgGS1-COD* and *DgGS1-UTR* hybridized strongly to the senescent infected cells (Fig. 3, G and H). Starch grains in the Frankia-infected tissue served as a marker for metabolic changes associated with senescence, since starch grains are not found in active, Frankia-infected nodule tissue.

Datisca Root Nodules Contain a Major Cytosolic GSPolypeptide and Lesser Amouns of a Plastidic Isoform

Immunoblots of nodule extract-SDS (SDS-polyacrylamide) electropherograms (Fig. 4) displayed two single bands representing GS subunits. The mass of the major polypeptide band (43 kD) was slightly larger than the predicted monomer from the translated amino acid sequence of *DgGS1-1* (39 kD). This major nodule polypeptide band corresponded to the single band observed in the root extracts (Fig. 4) and falls within the reported molecular-mass range of cytosolic GS subunits (Forde and Cullimore, 1989). A GS polypeptide band of higher mass (46–47 kD) was also detected at low levels in the nodule extracts, which corresponded in the gel to the major GS band in the Datisca leaf extracts, and which falls within the molecular mass range of plastidic GS isoforms. Somewhat slow migration rates in the protein blot relative to predicted polypeptide size may be related to compounds from the nodule extract, differences in percentage of SDS or gel thickness, or buffers used for the extracts and the standards; we do not believe that they represent a significant difference between the masses of *D. glomerata* GS subunits and enzyme from other plant sources. The 43-kD band could include more than one GS1 isoform with similar molecular mass; no doublet band was observed, however, that would indicate the presence of a nodule-specific isoform of different molecular mass, such as the γ isoform of GS1 observed in nodules of some determinate legumes (Bennett and Cullimore, 1989). The *D. glomerata* leaf extracts contained primarily the higher-molecular-mass GS isoform but also contained a lesser amount of the subunit corresponding to the cytosolic isoform. The polyclonal antibodies cross-reacted with both GS isoforms.

GS Protein Has the Same Nodule Localization Pattern as the Transcript

With the same antibodies as those used in the protein blot, GS protein in *D. glomerata* nodules was localized distinctly to the uninfected cortical tissue, and therefore showed the same spatial pattern as that observed for *DgGS1-1* transcripts (Fig. 3I). In uninfected cortical parenchyma cells, the green fluorescing fluorescein isothiocyanate (FITC)-signal of the secondary antibody was restricted to the cytoplasm and appeared also slightly accumulated around amyloplasts (Fig. 3J). GS hybridization signal was not detected in the Frankia-infected tissue, in the nodule periderm, or in the central vascular cylinder (Fig. 3I).

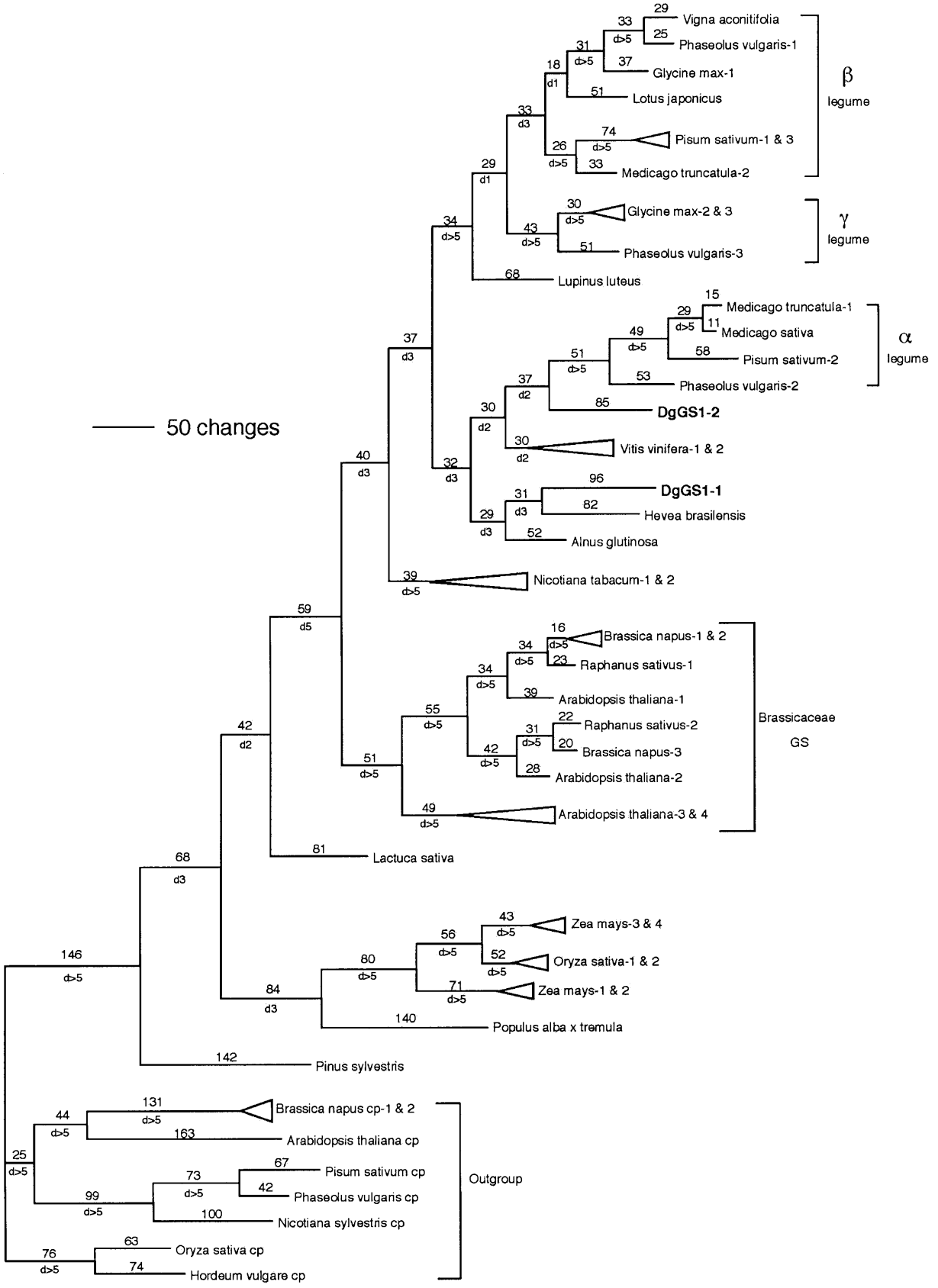

Figure 2. (*Legend appears on the following page.*)

No FITC-fluorescent signal was detected in control sections lacking primary antibody (Fig. 3K).

GS Enzyme Specific Activity Is Not Elevated in Nodules as Compared to Roots

Extracts of leaves, nodule-free roots, and nodules all had substantial amounts of GS activity. As shown in Table I, the specific enzyme activities (units per gram protein) were similar in all three organs.

Arg Is a Major Nodule Amino Acid

Amino acids were analyzed in extracts from nodule, root, leaf, and stem exudates (xylem sap), as well as from Frankia cells fractionated from the *D. glomerata* nodule tissue (Table II). In the root nodule extract, the three major amino acids were Gln, Arg, and Glu. In root tissue, leaf, and xylem sap, Gln, Glu, and Asp were the major amino acids; Arg was present only at low levels compared with Gln or Glu. Gln was the major transport amino acid in the xylem sap, as reported previously (Wheeler and Bond, 1970).

In extracts prepared from a nodule fraction enriched for Frankia, the major amino acids were Asp and Ser, with lesser proportions of Ala, Gly, and Glu (Table II). Ser and Gly were markedly higher in Frankia than in the nodule as a whole, especially as a fraction of the respective amino acid pools. Ornithine was also present at high levels compared with nodule tissue. Glu and Gln, by contrast, were markedly less abundant in the Frankia extracts than in the whole nodule extracts.

DISCUSSION

Primary assimilation of fixed nitrogen in the root nodules of *D. glomerata* has a novel spatial organization. Plant GS protein was not detected in the Frankia-infected sector of *D. glomerata* root nodules by an antibody that recognizes both GS1 and GS2 in a range of plant taxa (Bennett and Cullimore, 1989). Transcripts hybridizing either to the conserved coding region (*DgGS1-COD*) or to the 3′ UTR of *DgGS1-1*, a cDNA with high sequence homology to plant cytosolic GS genes that is expressed abundantly in *D. glomerata* root nodules, also were not detectable in the infected sector, with the exception of low-level gene expression in a band of early nitrogen-fixing cells and in senescent infected cells. Instead, high levels of both GS mRNA and protein were found in the surrounding uninfected tissue.

This partitioning of plant GS in the uninfected cortical tissue, at a distance from the locus of nitrogen fixation, contrasts markedly with the high levels of GS expression observed at sites of assimilation of recently fixed N, located in the central infected zone in legume nodules (Miao et al., 1991; Temple et al., 1995; Carvalho et al., 2000) or in infected nodule cortical cells of the actinorhizal plant, *A. glutinosa* (Guan et al.,

Figure 2. Single most parsimonious tree obtained by phylogenetic analysis of cytosolic GS sequences (consistency index [excluding autapomorphies] = .2604; retention index = .5717; rescaled consistency index = .1591). Plastidic GS sequences were designated as the outgroup. Numbers above the branches are branch lengths (ACCTRAN optimization); numbers below the branches preceded by "d" are decay values. Brackets with Greek letters refer to legume GS subclasses alpha, beta, and gamma. For graphical simplification, triangles are used to represent species pairs. Sources of Gln synthetase DNA sequences for phylogenetic analysis: organism, type (cp, plastidic localization; cyt, cytosolic localization), organ from which the cDNA was isolated for cytosolic GS sequences, GenBank accession number, reference. *A. glutinosa*, cyt (nodule), Y08681, Guan et al., 1996; Arabidopsis cp, S69727, Peterman and Goodman, 1991; Arabidopsis 1 cyt (genomic sequence derived mRNA) NM 105291; Arabidopsis 2 cyt (genomic sequence derived mRNA) BT000753; Arabidopsis 3 cyt (genomic sequence derived mRNA) BT006245; Arabidopsis 4 cyt (genomic sequence derived mRNA) AY128749; *Brassica napus-1*, cyt (root), X76736, Schock et al., 1994; *B. napus-2*, cyt (root), Y12459, Ochs et al., 1999; *B. napus-3*, cyt (root), X82997, Ochs et al., 1999; *B. napus cp-1*, cp, Y12458, Ochs et al., 1999; *B. napus cp-2*, cp, X72751, Ochs et al., 1999; *Glycine max*, cyt (nodule), S46513, Miao et al., 1991; *G. max*-1, cyt (nodule), X81460, Marsolier et al., 1995; *G. max*-2, cyt (nodule), X81700, Marsolier et al., 1995; *Hevea brasilensis*, cyt (latex cells), AF003197, Pujade-Renaud et al., 1997; *Hordeum vulgare*, cp, X16000, Freeman et al., 1990; *Lactuca sativa*, cyt (seed), X60092, Sakamoto et al., 1990; *Lotus japonicus*, cyt (root), X94299, Ruiz et al., 1999; Lupinus luteus, cyt (nodule), X71399, Boron and Legocki, 1993; *Medicago truncatula-1*, cyt (nodule), Y10267, Carvalho et al., 1997; *M. truncatula-2*, cyt (nodule), Y10268, Carvalho et al., 1997; *M. sativa*, cyt (nodule), U15591, Temple et al., 1995; *Nicotiana plumbaginifolia*, cp, M19055, Tingey and Coruzzi, 1987; *Nicotiana sylvestris*, cp, X66940, Becker et al., 1992; *Nicotiana tabacum-1*, cyt (seedling), X95932, Dubois et al., 1996; *N. tabacum-2*, cyt (seedling), X95933, Dubois et al., 1996; *Oryza sativa*, cyt (shoot), X14245, Sakamoto et al., 1989; *O. sativa*, cyt (derived from genomic sequence), AB037595, Kojima et al., 2000; *O. sativa*, cp, X14246, Sakamoto et al., 1989; *Pinus sylvestris*, cyt (seedling), X74429, Elmlinger et al., 1994; *Pisum sativum-1*, cyt (nodule), X05515, Tingey et al., 1987; *P. sativum-2*, cyt (nodule), X04763, Tingey et al., 1987; *P. sativum 3* cyt (nodule) M20663, Tingey et al., 1988; *P. sativum cp*, M20664, Tingey et al., 1988; *Phaseolus vulgaris-1*, cyt (root), X04001, Gebhardt et al., 1986; *P. vulgaris-2*, cyt (root), X04002, Gebhardt et al., 1986; *P. vulgaris*, cp, X12738, Lightfoot et al., 1988; *P. vulgaris gamma*, cyt (nodule) X14605, Bennett et al., 1989; *Populus alba* × *Populus tremula* cyt AF236074, Wu, D. and Kirby, E.G. direct submission, 2000; *Raphanus sativus-1*, cyt (senescing cotyledon), D25325, Watanabe et al., 1994; *R. sativus-2*, cyt (senescing cotyledon), D25326, Watanabe et al., 1994; *Vigna aconitifolia*, cyt (nodule), M94765, Lin et al., 1995; *Vitis vinifera-1*, cyt (shoot), X94321, Loylakakis and Roubelakis, 1996; *V. vinifera-2*, cyt (shoot), X94320, Loylakakis and Roubelakis, 1996; *Zea mays-1*, cyt (leaves), D14578(GS1C), Sakakibara et al., 1992; *Z. mays-2*, cyt (leaves), D14579(GS1D), Sakakibara et al., 1992; *Z. mays-3*, cyt (leaves), D14577(GS1B), Sakakibara et al., 1992; *Z. mays-4*, cyt (leaves), D14576(GS1A), Sakakibara et al., 1992.

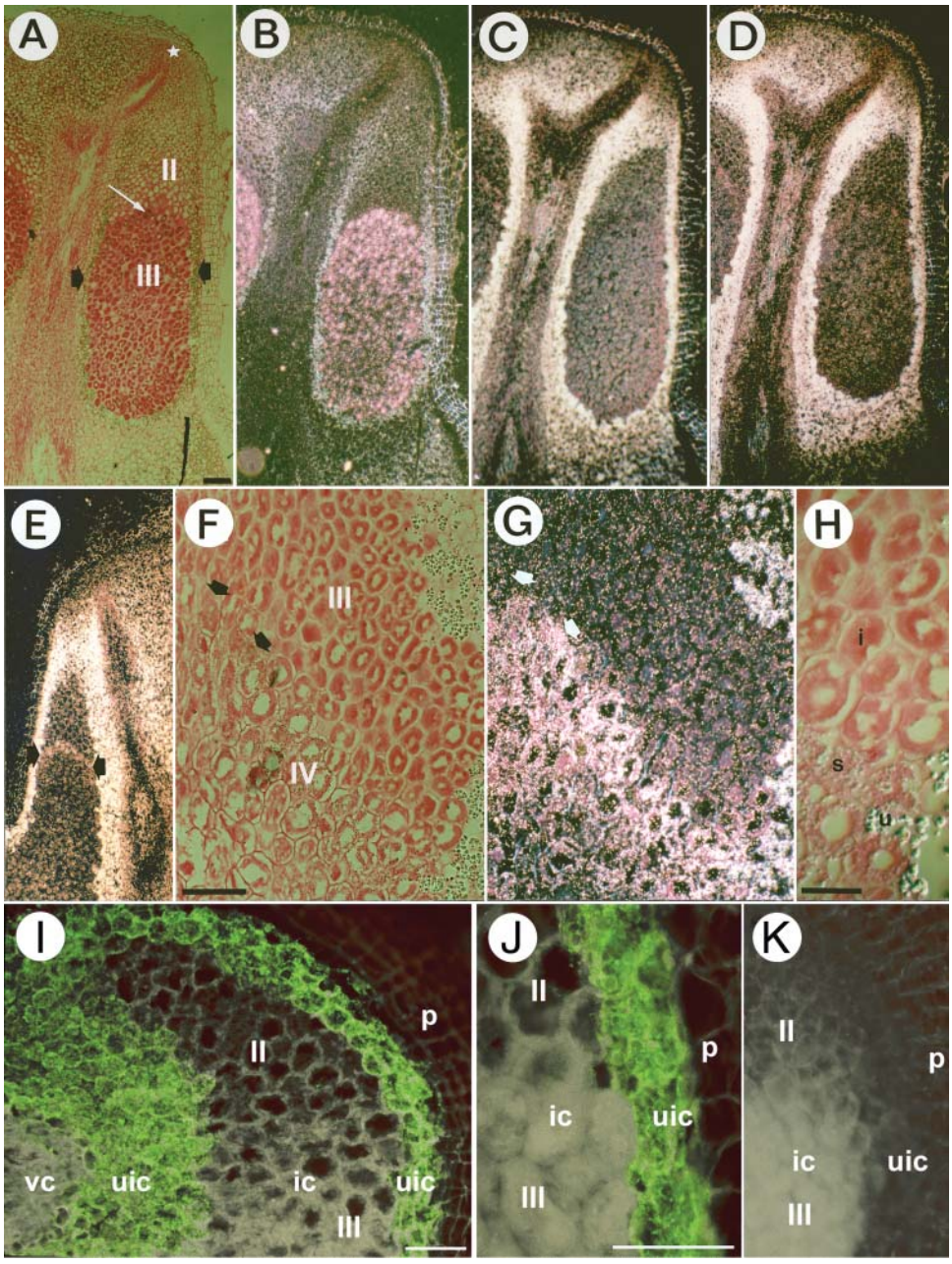

Figure 3. In situ localization of *DgGS1-COD*, *DgGS1-UTR*, and *nifH* mRNA; and immunolocalization of GS protein in longitudinal tissue sections of *D. glomerata* root nodules. A to I, In situ localization of mRNA. A, F, and H are brightfield images in which silver grains denoting hybridization are visible as black dots. B, C, D, E, and G are darkfield images in which silver grains appear as white or pinkish-white dots. Note that the cell walls of periderm and uninfected cortex (B) are birefringent in the polarized-light optics, as well as starch grains in the uninfected cortex. Scale bar in A represents 500 μm (valid for A to E). Scale bar in F represents 200 μm (valid for F and G). Scale bar in H represents 100 μm. A to D show a series of adjacent sections hybridized with different antisense RNA probes. A and B, Hybridization with Frankia *nifH*. The nodule lobe meristem in A is marked by a white star. Short black arrows point to the layers of uninfected cells containing large starch grains that surround the zone of infected cells. The white arrow points to an infected cell in the zone where nitrogen fixation was first detected, as denoted by Frankia *nifH* expression. The infection zone (II) and the nitrogen fixation zone (III) of the infected area are labeled in A. C, Hybridization with part of the coding region of *D. glomerata* Gln synthetase (*DgGS1-COD*). No signal above background was found in the nodule meristem, in the infected cells or in the vascular system of the nodule. High *DgGS1-1* expression was detected in the uninfected cells surrounding the patches of infected cells. Periderm birefringence due to epipolarization indicates unlabeled background for nodule tissues including uninfected cortex. Unlabeled background levels can also be seen by examining birefringent tissues in B, or the lignified (birefringent) xylem elements in C and D, which are dead cells lacking gene expression. D, Hybridization with the 3′ UTR of *D. glomerata* Gln synthetase (*DgGS1-UTR*). No significant difference was observed between the expression patterns of the two probes. E, Hybridization with *DgGS1-UTR*. Expression is detected mainly in

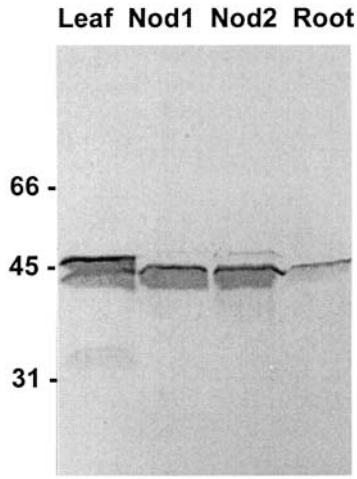

Figure 4. Immunoblot of SDS-PAGE of extracts of *D. glomerata* leaves, nodules, and roots, showing the subunits of GS detected by a polyclonal antibody raised against the *Phaseolus vulgaris* enzyme. The nodules marked "1" were 6 weeks old; the nodules marked "2" were 12 weeks old. The molecular masses (kD) at the left represent the positions of serum albumin, ovalbumin, and carbonic anhydrase run on the same electropherogram, blotted onto the same membrane, then cut off and stained separately. The amounts of protein loaded on each lane were: leaves, 44.2 μg; nodules 1, 33.2 μg; nodules 2, 33.0 μg; and roots, 9.75 μg. Each lane represented the extract from the following weight of tissue: leaves, 4.8 mg; nodules 1, 4.2 mg; nodules 2, 4.2 mg; and roots, 9.5 mg.

1996). Moreover, *DgGS1-1* expression was not detectable in the vascular tissue of *D. glomerata* nodules, nor was GS protein apparent, even though Gln is one of the major xylem transport amino acids. These findings indicate that the uninfected cortical tissue may play a central role in nitrogen processing for export in the Datisca nodule type. In amide-exporting legume nodules by contrast, a cytosolic GS isoform is expressed at high levels in the vascular bundles (Carvalho et al., 2000), where presumably GS-mediated reassimilation of fixed N for export takes place. In *A. glutinosa*, GS is abundantly expressed in the multilayered pericycle of the central vascular cylinder (Guan et al., 1996). GS is also expressed in the vascular tissue of plant organs other than nodules (Dubois et al., 1996).

In protein gels of *D. glomerata* nodule extracts, the finding of a single major band at 43 kD corresponding to the root GS band corroborates the likelihood that *DgGS1-1* encodes a root cytosolic GS isoform (Forde and Cullimore, 1989). A GS polypeptide with gel-migration behavior similar to the predominant leaf GS subunit is also present in the *D. glomerata* root nodules at low levels, probably corresponding to the plastidic GS isoform. A plastidic GS polypeptide at low abundance also occurs in some legume nodules (Bennett and Cullimore, 1989) and roots (Woodall et al., 1996).

Based on the GS phylogenetic analysis, *DgGS1-1* clearly belongs among the cytosolic sequences, where it is most closely allied with GS from nonnodulating *H. brasilensis* (rubber) and the actinorhizal species *A. glutinosa* but is part of a larger clade that includes the α subclass of legume GS sequences. *DgGS1-2*, apparently a low-abundance nodule GS isoform, is possibly even more closely allied with the legume α subclass. Differences between our analysis and previous GS phylogenetic analyses (Biesiadka and Legocki, 1997; Mathis et al., 2000; Morey et al., 2002) are primarily due to the inclusion of several nonlegume sequences in our data set.

There is not a close correlation between the phylogenetic grouping of the cytosolic GS sequences from the two actinorhizal species, *D. glomerata* and *A. glutinosa*, and their tissue localization patterns in the nodule; in Datisca, *DgGS1-COD* expression was confined to the uninfected nodule cortical cells, whereas in *A. glutinosa* nodules, GS was expressed highly in the infected cells and in the vascular tissue (Guan et al., 1996) but not in the uninfected cortical cells. The lack of correlation between nodule tissue localization and molecular phylogeny supports the contention of Doyle (1991) that the tissue specificity of GS gene expression is not a uniformly useful predictor of orthology. It suggests also that the novel tissue localization pattern in *D. glomerata* nodules reflects a difference in regulation, rather than in the structure of the gene or protein.

What is the basis for the novel expression pattern of cytosolic GS in *D. glomerata* root nodules, and how is GS tissue localization related to the organization of nodule nitrogen assimilation? The protein localization pattern in the nodule shows that no plant GS is unaccounted for in the infected tissue of the nodule, since the antibodies used for GS localization cross-react with the root (cytosolic) and leaf (plastidic)

Figure 3. (*continued.*)
the uninfected cortical tissue as in D. In some nodules, very low levels of *DgGS1-1* expression were detectable in infected cells at the onset of nitrogen fixation, as shown in E. F and G, Hybridization with *DgGS1-COD*. Detail of the older part of a nodule where some senescence of infected cells was observed. The nitrogen fixation zone (III) and the zone of senescence (IV) of infected cells are labeled. Expression of *DgGS* is found in the senescent infected cells (arrows). At the upper right in F and G, large starch grains are visible in uninfected cortical cells adjacent to the infected zone; smaller starch grains are present in the senescent infected cells. H, Detail of F Nitrogen-fixing infected (i), senescent infected (s), and uninfected (u) cells can be distinguished. I to L, GS protein immunolocalized in *D. glomerata* root nodules. I, In nodule tissue, the strong green FITC-fluorescence signal indicating the presence of GS was exclusively observed in uninfected cells (uic). GS was absent in immature (zone II) and mature (zone III) infected cells (ic), in the periderm (p) and in central vascular cylinder (vc). Scale bar in I represents 100 μm, valid for I and K. J, Detail of infected (ic; zone III) and peripheral uninfected (uic) nodule parenchyma cells. The green FITC-fluorescence signal is restricted to uninfected cells. Scale bar in J represents 50 μm. K, Control. The green FITC-fluorescence signal is absent when the primary antibody is replaced by phosphate-buffered saline (PBS).

Table I. *GS activity[a] in extracts of D. glomerata*

Plant Organ	Specific Activity
	μmol min^{-1} mg^{-1} protein
Leaf	0.86 ± 0.52
Nodule (6 week)	0.93 ± 0.41
Nodule (12 week)	1.11 ± 0.03
Root	1.05 ± 0.33

[a]Transferase activity measures the synthesis of γ-glutamyl hydroxamate from L-Gln and hydroxylamine in the presence of ADP, Mn_2^+, and Na arsenate. Values are means ± SE of two extractions, each assayed in duplicate.

isoforms in *D. glomerata*, as in a wide range of other plant taxa (Bennett and Cullimore, 1989). The GS protein localization is strongly reinforced by the nodule mRNA in situ hybridization, using a probe derived from a highly conserved part of the GS1 coding region (*DgGS1-COD*). Moreover, the same in situ hybridization pattern as with *DgGS1-COD* or *DgGS1-UTR* was obtained in *D. glomerata* nodules when a heterologous GS1 probe derived from *A. glutinosa* nodules was used (Pawlowski et al., 2003). Although the expression of additional GS1 gene homologs in *D. glomerata* nodules cannot be completely excluded, our findings taken together indicate that if present, expression levels of additional homologs are unlikely to be abundant, and the gene products are not localized to the infected tissue.

The absence of detectable GS in *D. glomerata* infected tissue may be due to metabolic regulation of gene expression by the particular nitrogen compounds released by Frankia into the host cytoplasm. The band of cells in the infected tissue expressing GS coincides with the earliest expression of *nifH*. In nodules of *A. glutinosa*, where the spatial and temporal expression of plant GS coincides with *nifH* expression, Guan et al. (1996) suggested that GS expression in this actinorhizal host is largely ammonium regulated. Ammonia efflux from rhizobial bacteroids has long been regarded as the major nitrogen transfer mechanism in legume symbioses (O'Gara and Shanmugam, 1976). Ammonium is one factor regulating cytosolic GS expression in legume nodules (Hirel et al., 1987; Stanford et al., 1993; Morey et al., 2002), as well as in nonsymbiotic plant tissue (Sukanya et al., 1994). *D. glomerata* GS is also expressed in the senescing portion of the infected tissue (Fig. 3G), where protein degradation and ammonium release would be expected to occur, further suggesting that in the presence of ammonium, GS would be expressed in the infected tissue of Datisca nodules. The lack of GS in mature nitrogen-fixing cells of *D. glomerata* nodules therefore suggests that ammonia efflux is not the primary means of delivering nitrogen from Frankia into the host tissue.

If ammonia is not the major N compound transferred by Frankia into mature infected host tissue, then N must be transferred primarily by amino acid efflux. In soybeans (*Glycine max*), a substantial fraction of fixed nitrogen can be assimilated in the Bradyrhizobium bacteroids via AlaDH and exported as Ala (Waters et al., 1998), and Ala is also secreted from pea bacteroids in addition to ammonia (Allaway et al., 2000). AlaDH and GDH activities have been detected in N_2-grown Frankia cultures in response to ammonium pulse (Berry et al., 1990; Schultz and Benson, 1990).

Table II. *Concentrations of amino acids (nmol [mg protein]$^{-1}$) in tissue extracts*

Data for nodules are means ± SE from two independent extracts; data for Frankia are means ± SE of four determinations from three independent extracts; data for root, sap, and leaf are from single preparations. Numbers in parentheses represent percent of the total amino acid pool. "Sap" is fluid expressed from stem sections by centrifugation. Extracted protein (mg/mL): nodule 0.66 ± 0.09; Frankia 0.045 ± 0.017; root 0.25; sap 0.88; leaf 0.78. nd, none detected.

	Nodule	Frankia	Root	Sap	Leaf
Ala	40 ± 4 (3)	61 ± 21 (8)	11 (4)	12 (12)	101 (4)
Arg	320 ± 101 (26)	47 ± 12 (6)	14 (5)	nd	32 (1)
Asn	trace	nd	12 (4)	nd	11 (0)
Asp	59 ± 9 (4)	99 ± 28 (14)	29 (10)	21 (21)	272 (10)
Cys	5 ± 2 (1)	nd	9 (3)	0.6 (1)	21 (1)
Gaba	82 ± 16 (7)	nd	31 (11)	6.3 (7)	266 (10)
Glu	209 ± 31 (17)	76 ± 2 (10)	46 (17)	28 (29)	543 (19)
Gln	401 ± 128 (33)	45 ± 8 (6)	81 (30)	15 (16)	1,160 (41)
Gly	9 ± 2 (1)	76 ± 24 (10)	10 (4)	3.8 (4)	41 (1)
His	19 ± 4 (2)	17 ± 1 (2)	nd	nd	14 (1)
Lys	9 ± 2 (1)	31 ± 4 (4)	nd	nd	16 (1)
Orn	1 ± 1 (0)	48 ± 7 (7)	5.4 (2)	1.3 (1)	nd
Ser	20 ± 2 (2)	152 ± 29 (21)	16 (6)	4.6 (5)	153 (5)
Thr	21 ± 1 (2)	51 ± 14 (7)	11 (4)	3.9 (4)	63 (2)
Val	8 ± 1 (1)	25 ± 1 (3)	nd	nd	41 (1)
Other[a]	≤8 (≤1)	nd	nd	nd	≤27 (≤1)

[a]Ile, Leu, Met, Phe, Pro, Trp, Tyr.

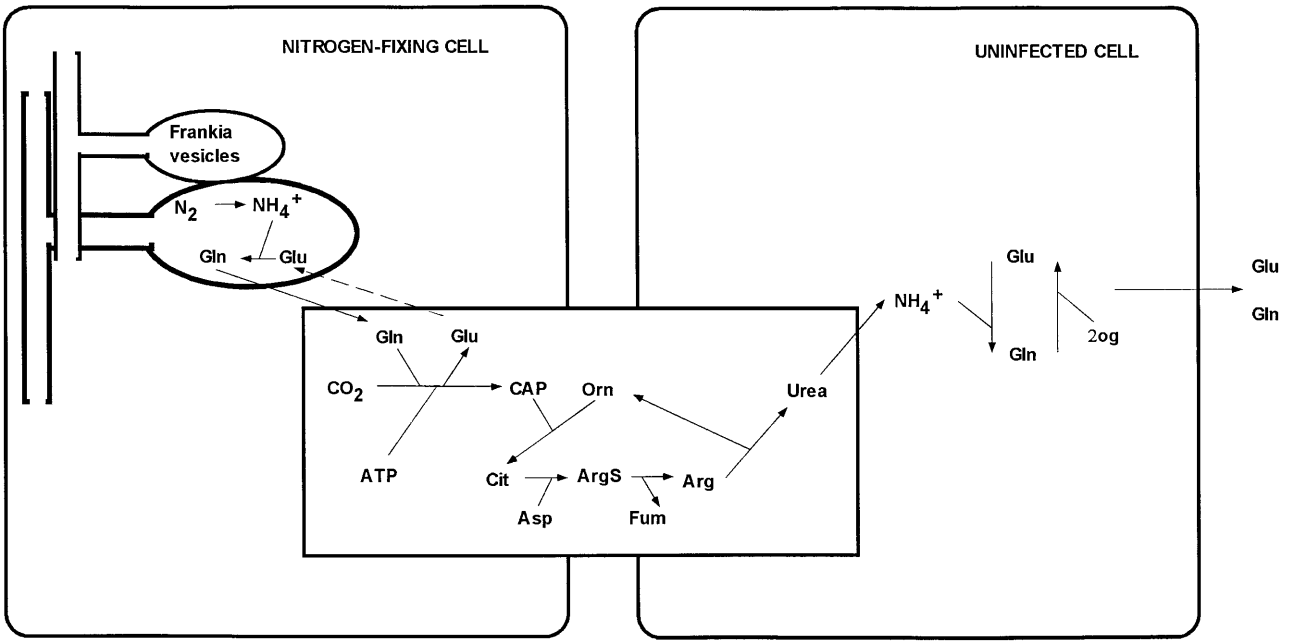

Figure 5. Model for nitrogen assimilation and export from root nodules of *D. glomerata*. The model assumes that primary ammonium assimilation occurs in the Frankia cells and that there is no free ammonium in the cytoplasm of the infected nodule cells. Arg is synthesized either in N-fixing cells for export or in uninfected cells for storage. In either case, Arg is catabolized by arginase and urease to release ammonium in uninfected cells, providing substrate for GS/GOGAT. Gln and Glu are then exported.

Lodwig et al. (2003) have provided evidence that both amino acid influx and efflux from bacteroids are fundamental to legume nodule N processing, even when ammonia is the main N excretion product. The relative contribution of ammonia versus amino acid efflux can be regulated by external conditions, as shown in soybean bacteroids, where Ala secretion is relatively higher at low oxygen partial pressure (Waters et al., 1998). In the Datisca/Coriaria nodule type, Frankia vesicles in mature cells are tightly packed inside a single symbiosome-like compartment, surrounded by a blanket of host mitochondria (Silvester et al., 1999), an arrangement that could be conducive to low oxygen partial pressures at the sites of nitrogen fixation, resulting in preferential amino acid efflux. Moreover, the Frankia genomic species infective on Datisca belongs to a 16S phylogenetic group that is distinct from Alnus-infective strains (Benson and Clawson, 2000). Little is known about the physiology of this group of frankiae, because as yet they cannot be cultured.

Root nodule nitrogen metabolism is a result of the interplay among primary assimilation, nitrogen storage, and nitrogen export from the nodule. To construct a unified model of nitrogen assimilation in *D. glomerata* nodules requires an understanding of how these functions are integrated among all the cellular and tissue compartments. In ureide-exporting legume nodules for example, there is a complex partitioning of metabolic functions between infected and uninfected nodule cortical tissues and among different organelles (Schubert, 1986). Information about amino acid pools in *D. glomerata* nodules can provide some clues about functional interactions. Total amino acid pools in *D. glomerata* nodules are not unlike those of the roots, with the major exception of Arg, which is an order of magnitude more abundant in nodules than in roots on a protein basis. Arg is not a major amino acid constituent of root nodules of legumes or of other actinorhizal genera (Wheeler and Bond, 1970). Citrulline, the precursor for Arg, is a major nodule amino acid in Alnus, and Arg has been reported to occur at low levels ($\leq$5% of total amino acids) in the nodules of several actinorhizal genera, including Alnus, Myrica, Ceanothus, Hippophae, and Elaeagnus (Leaf et al., 1958; Wheeler and Bond, 1970), indicating that portions of the Arg cycle are present in these actinorhizal symbioses. In Casuarina, Arg and citrulline occur abundantly in root xylem sap (Sellstedt and Atkins, 1991), but neither amino acid was detected in nodules of *Casuarina cunninghamiana* (Wheeler and Bond, 1970).

The one exception to this general pattern is to be found in nodules of *Coriaria myrtifolia* (Wheeler and Bond, 1970) where Arg represented 32% of total amino acids, Gln 24%, and Glu 23%, a nodule amino acid profile quite similar to that of *D. glomerata* reported here. Coriaria is phylogenetically very closely related to Datisca, both genera belonging to the Cucurbitales, and comparatively distant from the other major actinorhizal groups (Swensen, 1996). Moreover, Datisca

and Coriaria share a similar, distinctive nodule physiology and tissue arrangement (Silvester et al., 1999). The presence of abundant Arg in nodules compared with root and leaf tissues suggests that a specialized system of nitrogen storage and mobilization centered around Arg may function in Datisca and Coriaria nodules. Since Arg is apparently not transported out of the nodule at high levels, its catabolism may provide substrates in a nitrogen transport network between the uninfected and infected cortical tissue or in nitrogen recycling within the uninfected tissue. One product of Arg catabolism is free ammonium, via the urea cycle (Goldraij and Polacco, 2000). Since our GS localization studies indicate that free ammonium is unlikely to be present at high levels in the infected tissue, Arg degradation could take place in the uninfected cortical tissue. Such a pattern would explain the localization of host GS primarily in uninfected nodule cortical cells and the availability of Gln for export into the vascular system. Moreover, the cortical cells in the uninfected tissue are highly vacuolate compared to Frankia-infected cells and form a continuum between the infected zone and the vascular tissue, a likely location for a nitrogen processing network. A hypothetical assimilatory network involving amino acid export from Frankia and a urea cycle leading to Gln export is diagrammed in Figure 5.

The amino acid profile of symbiotic Frankia in *D. glomerata* nodules differs from that of the host tissue. Ser and Gly were particularly elevated in the Frankia extracts compared to total nodule amino acid pools, as was Orn. Gln and Glu pools on the other hand were unusually low in the symbiotic Frankia when compared either with the endogenous amino acid profile of free-living Frankia cultures that had been induced for nitrogen fixation (Berry et al., 1990) or with total nodule pools of *D. glomerata* (Table II). Ala similarly did not occur at notably high levels within the total Frankia amino acid pool. Thus if ammonia is assimilated in the symbiotic Frankia as Gln, Glu, or Ala, the activity of endogenous transferases and/or the amino acid export mechanism matches the rate of synthesis, even at low concentrations of these amino acids. In the only study to date of amino acid export from Frankia, Ser and lesser amounts of Gln were exported from an Alnus-infective Frankia strain induced in vitro for nitrogen fixation and exposed to a pulse of exogenous ^{13}N-ammonium (Berry et al., 1990).

CONCLUSION

The distinctive spatial localization pattern of GS protein and transcripts in *D. glomerata* root nodules suggests that the organization of metabolic and regulatory networks governing nitrogen assimilation represents a new variant type, compared with legumes or with *A. glutinosa*. Because of the complexity of nitrogen and carbon metabolism in the Datisca-Frankia nodule symbiotic system, we expect that isotopic labeling combined with NMR spectroscopy will be needed to clarify the successive steps in this unique organization of nitrogen assimilation. Such information will provide a basis for further exploration of the gene regulatory interactions of Frankia and the host in *D. glomerata* nodule nitrogen assimilation.

MATERIALS AND METHODS

Plant Material

Seeds of *Datisca glomerata* were collected in Gates Canyon, Vacaville, CA. *D. glomerata* plants were grown from seed in the greenhouse and inoculated with a slurry containing 0.5 g/plant of crushed nodules from *Ceanothus griseus* stock plants grown in aeroponics culture. Root nodules for mRNA isolation were harvested into liquid nitrogen at 4, 5, 7, and 11 weeks postinoculation (PI). Nodules for in situ hybridization were harvested at 6 to 10 weeks PI. For immunolocalization, nodules were harvested at 6 weeks PI. For protein analysis, leaves, nodules (6 weeks and 12 weeks PI), and roots (from uninoculated plants) were harvested. Harvested materials were in all cases used immediately or immediately frozen in liquid nitrogen and stored at −80°C. Nodule DNA, organ RNA, and mRNA isolation have been described in Okubara et al. (1999). For amino acid analysis, nodules were harvested from mature, nodulated plants as described for protein analysis.

Cloning of GS Sequences

For PCR amplification of GS sequences, primers were designed from two stretches of 100% amino acid conservation within the common GS coding regions of eight plant species (*α-GS1* and *β-GS1* from *Phaseolus vulgaris*, *GS1* from *Lactuca sativa*, cytosolic *GS* from *Vigna aconitifolia*, cytosolic *GS* from *Lupinus angustifolius*, *α-GS* from *Pisum sativum*, cytosolic *GS* from *Alnus glutinosa*, *GS1* from *Glycine max* roots, and *GS1* from *Nicotiana plumbaginifolia*). An 880-bp partial cDNA of *DgGS1-1* was amplified using the primers: 5′-CCIAARTGGAAYTAYGAYGG-3′ (*GS51*) and 5′-AAIACIACRTAIGGRTCCATRTT-3′ (GS32) and cloned in pGEM-T (Promega, Madison, WI). A 730-bp *Pst*I fragment representing nucleotide positions 227 to approximately 960 of the full-length cDNA was subcloned in pBluescript KS+ (Stratagene, La Jolla, CA), yielding p*DgGS1-COD*. Amplification of the 3′ untranslated portion of *DgGS1-1* was carried out using pooled nodule cDNA library DNA with T7 primer and a *GS*-specific primer (GS7): 5′-CATAAGTG GTCTGCTC-3′. The TAA at positions 3 through 5 in the GS7 primer encode the translational stop of *DgGS1-1*.

To obtain the second GS species (*DgGS1-2*), hand slices of Frankia-infected tissue from nodules 11 weeks PI were excised under a dissecting microscope and frozen in liquid nitrogen for RNA isolation. Poly(A) mRNA was isolated from the excised tissue using oligo(dT)$_{25}$ Dynabeads as recommended by the manufacturer (Dynal Biotech, Lake Success, NY). First-strand cDNA synthesis was carried out using Superscript II MMLV reverse transcriptase (Gibco BRL, Gaithersburg, MD), followed by PCR with primers *GS51* and *GS32*. The PCR product was cloned in pCRII (Invitrogen, Carlsbad, CA), mobilized into *Escherichia coli* strain INV*α*F′, and plasmid insert DNA was sequenced.

cDNA Library Screening

A Datisca nodule cDNA library was constructed from equal amounts of mRNA from nodules harvested at 4-, 7-, and 11-weeks PI, as described in Okubara et al. (1999), with an average insert size of 1.6 kb. Approximately 166,000 recombinant phage clones from the nodule cDNA library were hybridized (Sambrook and Russell, 2000) to radiolabeled *DgGS1-COD*. Four clones with inserts of 1.5 to 1.7 kb of the 32 positives that strongly hybridized to *DgGS1-COD* were sequenced. All were identified as *DgGS1-1*. A full-length cDNA clone of *DgGS1-1* was selected from these on the basis of insert size and nucleotide sequence (GenBank accession no. AY422224). In a separate screen, about 120,000 recombinant phage clones were hybridized to an 880-bp probe consisting of the *DgGS1-2* partial coding region (GenBank accession no. AY422225). Twenty-three candidate phage clones were further purified (secondary screen). Four clones that had inserts of approximately 1.5 to 1.7 kb were selected for phagemid excision and nucleotide sequencing.

In Situ Hybridization

For in situ hybridization, ^{35}S-labeled antisense and sense RNA probes were prepared from the internal cDNA fragment of *DgGS1-1*, designated *DgGS1-COD*, in pBluescript KS+. For production of antisense RNA, p*DgGS1-COD* was linearized with *Xba*I and transcribed with T3 RNA polymerase (Life-Technologies, Gaithersburg, MD) in the presence of ^{35}S-UTP (Amersham Pharmacia Biotech, Uppsala). For the production of sense RNA, p*DgGS1-COD* was linearized with *Eco*RI and transcribed with T7 RNA polymerase (Life-tech). For production of the gene-specific probe *DgGS1-UTR*, the 307-bp fragment representing the entire UTR of the cDNA was amplified by PCR and cloned in pGEM-T (Promega), yielding p*DgGS1-UTR*. For production of antisense RNA, p*DgGS1-UTR* was linearized with *Sal*I and transcribed with T7 RNA polymerase in the presence of ^{35}S-UTP. The preparation of a Frankia *nifH* antisense probe has been described (Ribeiro et al., 1995). Because a full-length cDNA of *DgGS1-2* was not obtained in the library screen, such that *DgGS1-2* was expected to cross-hybridize with *DgGS1-COD*, in situ hybridization with this sequence as probe was not carried out.

Root nodules were harvested at 6 to 9 weeks PI (3–6 weeks post nodule initiation) and fixed intact in 4% paraformaldehyde, 0.25% glutaraldehyde in sodium phosphate buffer, pH 6.9 for 2 h under vacuum and embedded in paraffin as described by van de Wiel et al. (1990). Seven- to ten-micrometer thick sections were cut and placed on polylysine coated slides. Slides containing adjacent sections were used for the three different probes. In situ hybridization was performed as described by van de Wiel et al. (1990) with modifications according to Ribeiro et al. (1995). After washing, the slides were coated with microautoradiography emulsion LM-1 (Amersham) and exposed for 4 weeks at 4°C. They were developed in Kodak D19 developer (Eastman Kodak, Rochester, NY) and fixed in Kodak fix. Sections were counterstained with 0.02% ruthenium red and 0.025% toluidine blue O for 5 min each and mounted with DePeX (BDH Laboratory Supplies, Poole, UK).

RNA Gel Blots

DgGS1-COD (the *DgGS1-1* internal fragment) and the *DgGS1-2* partial cDNA were labeled with ^{32}P and used as probes of total mRNA isolated from leaf, (green) flowers, and (green) developing fruits, as well as total mRNA from nodules harvested at 6 weeks after inoculation. Total RNA from clone pTa71 (Gerlach and Bedbrook, 1979), which contains a 9-kb *Eco*RI fragment of *Triticum aestivum* consisting of the 18S-5.8S-25S rRNA genes and nontranscribed spacer sequences, was used as a positive control. The RNA samples were separated on 1.2% formaldehyde gel (Sambrook and Russell, 2000) and blotted onto Hi-Bond XL according to instructions of the manufacturer (Amersham). Hybridization was carried out at 65°C, and washing conditions were as described previously (Okubara et al., 1999): blots were washed in 2× SSC, 0.5× SSC, and 0.1× SSC once each for 15 min; and in 0.1% SDS at room temperature. Autoradiography was carried out on preflashed film at −80°C for 6 d. Phosphoimaging and normalization of the experimental probe hybridization in relation to the rRNA hybridization was done using Fuji FLA-3000 and software program TINA 2.0 (Raytest, Sprockhövel, Germany).

Phylogenetic Analysis

The *D. glomerata* DNA sequences from clone *DgGS1-1* and *DgGS1-2* were compared to other plant GS genes through phylogenetic analysis. The *DgGS1-1* sequence used for comparison was a 1,071 bp portion of the GS cDNA in the coding region and did not include any 3′ or 5′ UTRs. For *DgGS1-2*, the entire partial cDNA (880 bp) was used. A total of 47 different DNA sequences encoding both cytosolic and chloroplast GS were obtained from GenBank (Fig. 2) and aligned to each other and to the *D. glomerata* sequences. The alignment was accomplished using ClustalW (Thompson et al., 1994) with the gap opening penalty set at 15 and the gap extension penalty set at 6.66. The computer-generated alignment was then manually edited. The aligned data set was analyzed using a parsimony-based heuristic search with 1,000 replications and tree bisection-reconnection branch swapping (PAUP*4.0b4a; Swofford, 1998). Gaps were treated as missing data. Based on our own preliminary analyses and upon previously published analyses (Doyle, 1991; Kumada et al., 1993; Biesiadka and Legocki, 1997), the outgroup comprised eight sequences encoding chloroplast GS from various plant species. The strength of support for individual branches in the tree was estimated using decay indices (Bremer, 1988; Donoghue et al., 1992). Decay analysis was implemented by repeating the original heuristic search and saving all trees up to five steps longer than the shortest tree found by the initial search. The number of additional steps required for the collapse of various branches was determined by inspecting consensus trees constructed from trees found at each length and all those shorter.

GS Protein Analysis

Samples of leaves, root nodules (6 weeks or 12 weeks old), and nodule-free roots were frozen at −80°C then ground in a mortar, first with liquid nitrogen, then extracted with a buffer that contained 10 mM Tris-Cl, pH 7.5, 5 mM Glu, 10 mM $MgCl_2$, 10% glycerol, 1 mM dithiothreitol (DTT), 0.1% mercaptoethanol, 0.05% Triton X-100, and 0.02 mM phenylmethylsulfonylfluoride, adapted from Bennett and Cullimore (1989). For leaves and nodules, 0.5-g samples were ground in 4 mL of buffer; for roots, 2-g samples were ground in 6 mL of buffer. Cell debris was removed by centrifugation. Protein concentrations were measured by dye binding (Bradford, 1976).

Crude extracts were subjected to SDS-polyacrylamide electrophoresis according to Laemmli (1970) and transferred to nitrocellulose membranes. Immunodetection of Gln synthetase was performed according to Sambrook and Russell (2000), using rabbit antiserum directed against *P. vulgaris* nodule Gln synthetase (2 μg mL^{-1} of lyophilized enzyme, preparation kindly provided by J.V. Cullimore; see Bennett and Cullimore, 1989), goat anti-rabbit-IgG conjugated to alkaline phosphatase (Sigma, St. Louis), 5-bromo-4-chloro-3-indolyl phosphate (Sigma), and nitroblue tetrazolium (Eastman Kodak) to visualize bands. The GS antibody cross-reacts with both GS1 and GS2 in a wide range of plants (Bennett and Cullimore, 1989).

The transferase activity of Gln synthetase was measured following the procedure of Cullimore and Sims (1980). The assay mixture contained 100 mM Tris-acetate, pH 6.4, 100 mM L-Gln, 60 mM hydroxylamine, 1 mM ADP, 2 mM $MnCl_2$, and 40 mM sodium arsenate, an amount of protein extract ranging from 4 to 16 μg (roots) to 18 to 72 μg (leaves) in 1 mL. The mixtures were incubated at 20°C for 30 min; then the reaction was stopped, and the relative amount of glutamyl hydroxamate was estimated by the addition of 1.5 mL of a solution containing 4% (0.24 M) trichloroacetic acid and 3.2% (0.2 M) $FeCl_3$ in 0.5 M HCl (Ferguson and Sims, 1969). Background values from reactions without enzyme were subtracted from the enzyme-catalyzed values.

Immunolocalization of Nodule GS Protein

Datisca root nodules were fixed at 6 weeks PI in 4% paraformaldehyde and 0.1% glutaraldehyde in 50 mM potassium phosphate buffer, pH 6.9, overnight at 4°C. Fixed tissue was rinsed in buffer and stored in buffer with sodium azide at 4°C before use. Nodules were embedded in HistoPrep (Fisher, Loughborough, UK), cooled in liquid nitrogen, and stored after embedment at −80°C. Frozen sections were cut with a Cryocut 1800 (Leica Microsystems, Vienna) at (−)19°C, knife angle 0° to 3°. Twenty- to thirty-micrometer thick sections were transferred to slides at room temperature, and dried at least 5 s. Polyclonal antibodies against plant GS were obtained courtesy of J.V. Cullimore, as described above for protein blots. Preparatory blots were done prior to incubation to determine the optimal range of concentration of the primary antibody. Tissue sections were incubated in blocking buffer (1% non-fat dry milk in 1 × PBS) for 1 h prior to incubation in primary antibody for 15 s. After rinsing in PBS, the sections were incubated with secondary antibody (goat anti-rabbit IgG conjugated with Alexa TM 488 [Molecular Probes, Eugene, OR] 2 g/mL) at 1:100 and 1:200 for 15 s and rinsed in PBS. As controls, the primary antibody was replaced by buffer followed by Alexa-conjugated secondary antibody in buffer (Fig. 3K) or by a different primary antibody also generated in rabbits, which hybridized to the infected tissue (data not shown). In a concentration series of the anti-GS antibody (1:100, 1:50, 1:25, 1:10), the localization pattern was consistent (i.e. hybridization to the infected tissue was not observed) even at the 1:10 dilution. Sections were mounted in 90% glycerol, 10% 1 × PBS containing 0.2% p-phenylenediamine (DeWitt and Sussman, 1995), viewed with an Olympus BH-2 with epifluorescence, using a B filter EY 455 (excitation 490) with a DM 500 barrier filter, and photographed with Kodak Elite II 400 film. To eliminate background yellow autofluorescence, yellow hues were digitally removed from Figure 3, I–K, in a global fashion.

Amino Acid Profiles

To quantify endogenous amino acid pools, extracts were prepared from several tissues of *D. glomerata* including whole nodule, leaf, stem exudates,

and nodule-Frankia cells. Tissues were either extracted fresh or frozen in liquid nitrogen at the time of harvest and stored at −80°C until use. Leaf, root and whole-nodule extracts for amino acid analysis were prepared by homogenization on ice in 50 mM Tris buffer, 200 mM Suc, 2 mM EDTA, 5 mM DTT, pH 8. Stem exudates from well-watered plants were collected early in the morning by microcentrifugation of small-diameter cut stems at 3,000 rpm for 5 min followed by 4,000 rpm for 5 min, using a swinging-bucket rotor. To obtain an extract enriched in Frankia cell amino acids, a differential filtration method was modified from Lundquist and Huss-Danell (1992). Nodules harvested 6 weeks PI were homogenized on ice in 50 mM Tris buffer, pH 8 (1 g nodule/30 mL buffer) or in 50 mM phosphate buffered saline, pH 7.4. The addition of Suc, DTT, or EDTA to the buffer made no difference in the amino acid profile. The resulting brei containing clusters of Frankia cells was filtered through 167-μm nylon mesh. The filtrate suspension was then filtered through 20-μm nylon mesh. The 20-μm retentate was resuspended in 1 to 3 mL buffer and sonicated on ice for 30 s, using a sonifier (Branson Ultrasonics, Danbury, CT) at 50% duty cycle, output setting 6. The sonicate was microcentrifuged at 15,000 rpm for 20 min at 4°C and the supernatant retained for analysis. Extracts from all the tissues were analyzed for amino acids on a Beckman 6300 Amino Acid Analyzer using Li citrate at the Molecular Structure Facility, University of California, Davis.

Novel Materials

Upon request, all novel materials described in this publication will be made available in a timely manner for noncommercial research purposes, subject to the requisite permission from any third-party owners of all or parts of the material. Obtaining any permissions will be the responsibility of the requestor.

Sequence data from this article have been deposited with the EMBL/GenBank data libraries under accession numbers AY422224 and AY422225.

ACKNOWLEDGMENTS

The technical assistance of Melinda Klein, Carolyn Woo, and Rochelle Jones is gratefully acknowledged. We also thank Judy Jernstedt for the kind use of laboratory facilities.

Received August 8, 2003; returned for revision April 14, 2004; accepted May 2, 2004.

LITERATURE CITED

Allaway D, Lodwig EM, Crompton LA, Wood M, Parsons R, Wheeler TR, Poole PS (2000) Identification of alanine dehydrogenase and its role in mixed secretion of ammonium and alanine by pea bacteroids. Mol Microbiol **36:** 508–515

Baker A, Parsons R (1997) Rapid assimilation of recently fixed N_2 in root nodules of *Myrica gale*. Physiol Plantarum **99:** 640–647

Becker TW, Caboche M, Carrayol E, Hirel B (1992) Nucleotide sequence of a tobacco cDNA encoding plastidic glutamine synthetase and light inducibility, organ specificity and diurnal rhythmicity in the expression of the corresponding genes of tobacco and tomato. Plant Mol Biol **19:** 367–379

Bennett MJ, Cullimore JV (1989) Glutamine synthetase isozymes of *Phaseolus vulgaris* L.: subunit composition in developing root nodules and plumulus. Planta **179:** 433–440

Bennett MJ, Lightfoot DA, Cullimore JV (1989) cDNA sequence and differential expression of the gene encoding the glutamine synthetase and polypeptide of *Phaseolus vulgaris* L. Plant Mol Biol **12:** 553–565

Benson DR, Clawson ML (2000) Evolution of the actinorhizal plant symbiosis. *In* ER Triplett, ed, Prokaryotic Nitrogen Fixation: A Model System for Analysis of a Biological Process. Horizon Scientific Press, Wymondham, UK, pp 207–224

Berry AM, Thayer JR, Enderlin CS, Jones AD (1990) Pattern of [^{13}N]ammonium uptake and assimilation by *Frankia* HFPAr13. Arch Microbiol **154:** 510–513

Biesiadka J, Legocki AB (1997) Evolution of the glutamine synthetase gene in plants. Plant Sci **128:** 51–58

Boron LJ, Legocki AB (1993) Cloning and characterization of a nodule-enhanced glutamine synthetase-encoding gene from Lupinus luteus. Gene **136:** 95–102

Bradford MM (1976) A rapid and sensitive method for the quantitation of microgram quantities of protein utilizing the principle of protein dye binding. J Biol Chem **72:** 248–254

Bremer K (1988) The limits of amino acid sequence data in angiosperm phylogenetic reconstruction. Evolution **42:** 795–803

Carvalho H, Lescure N, De Billy F, Chabaud M, Lima L, Salema R, Cullimore J (2000) Cellular expression and regulation of the *Medicago truncatula* cytosolic glutamine synthetase genes in root nodules. Plant Mol Biol **42:** 741–756

Carvalho H, Sunkel C, Salema R, Cullimore JV (1997) Heteromeric assembly of the cytosolic glutamine synthetase polypeptides of *Medicago truncatula*: complementation of a *glnA Escherichia coli* mutant with a plant domain-swapped enzyme. Plant Mol Biol **35:** 623–632

Cullimore JV, Sims AP (1980) An association between photorespiration and protein catabolism: studies with *Chlamydomonas*. Planta **150:** 392–396

DeWitt ND, Sussman MR (1995) Immunocytological localization of an epitope-tagged plasma membrane proton pump (H^+-ATPase) in phloem companion cells. Plant Cell **7:** 2053–2067

Donoghue MJ, Olmstead EJ, Smith JF, Palmer JD (1992) Phylogenetic relationships of Dipsacales based on *rbcL* sequences. Ann Mo Bot Gard **79:** 333–345

Doyle JJ (1991) Evolution of higher-plant glutamine synthetase genes: tissue specificity as a criterion for predicting orthology. Mol Biol Evol **8:** 366–377

Dubois F, Brugiere N, Sangwan RS, Hirel B (1996) Localization of tobacco cytosolic glutamine synthetase enzymes and the corresponding transcripts shows organ- and cell-specific patterns of protein synthesis and gene expression. Plant Mol Biol **31:** 803–817

Elmlinger MW, Bolle C, Batschauer A, Oelmuller R, Mohr H (1994) Coaction of blue light and light absorbed by phytochrome in control of glutamine synthetase gene expression in Scots pine (*Pinus sylvestris* L.) seedlings. Planta **192:** 189–194

Ferguson AR, Sims AP (1969) Inactivation in vivo of glutamine synthetase and NAD-specific glutamate dehydrogenase: its role in the regulation of glutamine synthesis in yeasts. J Gen Microbiol **69:** 423–427

Forde BG, Cullimore JV (1989) The molecular biology of glutamine synthetase in higher plants. Oxf Surv Plant Mol Cell Biol **6:** 247–296

Forde BG, Day HM, Turton JF, Wen-jun S, Cullimore JV, Oliver JE (1989) Two glutamine synthetase genes from *Phaseolus vulgaris* L. display contrasting developmental and spatial patterns of expression in transgenic *Lotus corniculatus* plants. Plant Cell **1:** 391–401

Freeman J, Marquez A, Wallsgrove RM, Saarelainen R, Forde BG (1990) Molecular analysis of barley mutants deficient in chloroplast glutamine synthetase. Plant Mol Biol **14:** 297–311

Gebhardt C, Oliver JE, Forde BG, Saarelainen R, Miflin BJ (1986) Primary structure and differential expression of glutamine synthetase genes in nodules, roots and leaves of *Phaseolus vulgaris*. EMBO J **5:** 1429–1435

Gerlach WL, Bedbrook JR (1979) Cloning and characterization of ribosomal RNA genes from wheat and barley. Nucleic Acids Res **7:** 1869–1885

Goldraij A, Polacco JC (2000) Arginine degradation by arginase in mitochondria of soybean seedling cotyledons. Planta **210:** 652–658

Guan C, Ribeiro A, Akkermans ADL, Jing Y, Van Kammen A, Bisseling T, Pawlowski K (1996) Nitrogen metabolism in actinorhizal nodules of *Alnus glutinosa*: expression of glutamine synthetase and acetylornithine transaminase. Plant Mol Biol **32:** 1177–1184

Hafeez F, Akkermans ADL, Chaudhary AH (1984) Observations on the ultrastructure of *Frankia* sp. in root nodules of *Datisca cannabina* L. Plant Soil **79:** 383–402

Hirel B, Perrot-Rechenmann C, Maudinas B, Gadal P (1982) Glutamine synthetase in alder (*Alnus glutinosa*) root nodules. Purification, properties and cytoimmunochemical localization. Physiol Plant **55:** 197–203

Hirel B, Bouet C, King B, Layzell D, Jacobs F, Verma DPS (1987) Glutamine synthetase genes are regulated by ammonia provided externally or by symbiotic nitrogen fixation. EMBO J **6:** 1167–1172

Jacobsen K, Berry AM (2002) Callose in *Frankia*-infected tissue of *Datisca glomerata* is an artifact of specimen preparation. Plant Biol **4:** 46–52

Kluge A, Farris JS (1969) Quantitative phyletics and the evolution of anurans. Syst Zool **18:** 1–32

Kojima S, Hanzawa S, Hayakawa T, Hayashi M, Yamaya T (2000) Nucleotide sequence of a genomic DNA (accession no. AB037664) and cDNA (accession no. AB037595) encoding cytosolic glutamine synthetase in Sasanishiki, a leading cultivar of rice in northern Japan (PGR00-048). Plant Physiol **122:** 1459

Kumada Y, Benson DR, Hilleman D, Hosted TJ, Rochefort DA, Thompson CJ, Wohlleben W, Tateno Y (1993) Evolution of the glutamine synthetase gene, one of the oldest existing and functioning genes. Proc Natl Acad Sci USA **90:** 3009–3013

Laemmli UK (1970) Cleavage of structural proteins during the assembly of the head of bacteriophage T4. Nature **227:** 680–685

Leaf G, Gardner IC, Bond G (1958) Observations on the composition and metabolism of the nitrogen-fixing root nodules of *Alnus.* J Exp Bot **9:** 320–331

Lightfoot DA, Green NK, Cullimore JV (1988) The chloroplast-located glutamine synthetase of *Phaseolus vulgaris* L.: nucleotide sequence, expression in different organs and uptake into isolated chloroplasts. Plant Mol Biol **11:** 191–202

Lin Z, Miao GH, Verma DP (1995) A cDNA sequence encoding glutamine synthetase is preferentially expressed in nodules of *Vigna aconitifolia.* Plant Physiol **107:** 279–280

Lodwig EM, Hosie AHF, Bourdes A, Findlay K, Allaway D, Karunakaran R, Downie JA, Poole PS (2003) Amino-acid cycling drives nitrogen fixation in the legume-*Rhizobium* symbiosis. Nature **422:** 722–726

Lundquist PO, Huss-Danell K (1992) Immunological studies of glutamine synthetase in *Frankia-Alnus* incana symbioses. FEMS Microbiol Lett **91:** 141–146

Loylakakis KA, Roubelakis-Angelakis KA (1996) Characterization of *Vitis vinifera* L. glutamine synthetase and molecular cloning of cDNAs for the cytosolic enzyme. Plant Mol Biol **3:** 983–992

Marsolier MC, Debrosses G, Hirel B (1995) Identification of several soybean cytosolic glutamine synthetase transcripts highly or specifically expressed in nodules: expression studies using one of the corresponding genes in transgenic *Lotus corniculatus.* Plant Mol Biol **27:** 1–15

Mathis R, Gamas P, Meyer Y, Cullimore JV (2000) The presence of GSI-like genes in higher plants: support for the paralogous evolution of GSI and GSII genes. J Mol Evol **50:** 116–122

Miao GH, Hirel B, Marsolier MC, Ridge RW, Verma DP (1991) Ammonia-regulated expression of a soybean gene encoding cytosolic glutamine synthetase in transgenic *Lotus corniculatus.* Plant Cell **3:** 11–22

Morey KJ, Ortega JL, Sengupta-Gopalan C (2002) Cytosolic glutamine synthetase in soybean is encoded by a multigene family, and the members are regulated in an organ-specific and developmental manner. Plant Physiol **128:** 182–193

Ochs G, Schock G, Trischler M, Kosemund K, Wild A (1999) Complexity and expression of the glutamine synthetase multigene family in the amphidiploid crop *Brassica napus.* Plant Mol Biol **39:** 395–405

O'Gara F, Shanmugam KT (1976) Regulation of nitrogen fixation by rhizobia: export of fixed nitrogen as ammonium ion. Biochim Biophys Acta **437:** 313–321

Okubara PA, Fujishige NA, Hirsch AM, Berry AM (2000) Dg93, a nodule-abundant mRNA of *Datisca glomerata* with homology to a soybean early nodulin gene. Plant Physiol **122:** 1073–1079

Okubara PA, Pawlowski K, Murphy TM, Berry AM (1999) Symbiotic root nodules of the actinorhizal plant *Datisca glomerata* express Rubisco activase mRNA. Plant Physiol **120:** 411–420

Padilla JE, Campos F, Conde V, Lara M, Sanchez F (1987) Nodule specific glutamine synthetase is expressed before the onset of nitrogen fixation in *Phaseolus vulgaris* L. Plant Mol Biol **9:** 65–74

Pawlowski K, Swensen S, Guan C, Hadri A, Berry AM, Bisseling T (2003) Distinct patterns of symbiosis-related gene expression in actinorhizal nodules from different plant families. Mol Plant Microbe Interact **16:** 796–807

Peterman TK, Goodman HM (1991) The glutamine synthetase gene family of *Arabidopsis thaliana*: light-regulation and differential expression in leaves, roots and seeds. Mol Gen Genet **230:** 145–154

Pujade-Renaud V, Perrot-Rechenmann C, Chrestin H, Lacrotte R, Guern J (1997) Characterization of a full-length cDNA clone encoding glutamine synthetase from rubber tree latex. Plant Physiol Biochem **35:** 85–93

Ribeiro A, Akkermans ADL, van Kammen A, Bisseling T, Pawlowski K (1995) A nodule-specific gene encoding a subtilisin-like protease is expressed in early stages of actinorhizal development. Plant Cell **7:** 785–794

Rubio LM, Ludden PW (2002) The gene products of the *nif* regulon. *In* J Leigh, ed, Nitrogen Fixation at the Millennium. Elsevier Science B.V., Amsterdam, pp 101–136

Ruiz MT, Prosser IM, Hirel B, Clarkson DT (1999) A cDNA sequence (Accession No. X94299) encoding a cytosolic subunit of glutamine synthetase in the model legume Lotus japonicus. Plant Physiol **119:** 1148

Sakakibara H, Kawabata S, Takahashi H, Hase T, Sugiyama T (1992) Molecular cloning of the family of glutamine synthetase genes from maize: expression of genes for glutamine synthetase and ferredoxin-dependent glutamate synthase in photosynthetic and non-photosynthetic tissues. Plant Cell Physiol **33:** 49–58

Sakamoto A, Ogawa M, Masumura T, Shibata D, Takeba G, Tanaka K, Fujii S (1989) Three cDNA sequences coding for glutamine synthetase polypeptides in *Oryza sativa* L. Plant Mol Biol **13:** 611–614

Sakamoto A, Takeba G, Shibata D, Tanaka K (1990) Phytochrome-mediated activation of the gene for cytosolic glutamine-synthetase (*GS1*) during imbibition of photosensitive lettuce seeds. Plant Mol Biol **15:** 317–323

Sambrook J, Russell DW (2000) Molecular Cloning: A Laboratory Manual. Cold Spring Harbor Laboratory Press, Cold Spring Harbor, NY

Schock G, Ochs G, Wild A (1994) Glutamine synthetase from roots of *Brassica napus*: nucleotide sequence of cytosolic isoform. Plant Physiol **105:** 757–758

Schubert KR (1986) Products of biological nitrogen fixation in higher plants: synthesis, transport and metabolism. Annu Rev Plant Physiol **37:** 539–574

Schultz NA, Benson DR (1990) Enzymes of ammonia assimilation in hyphae and vesicles of *Frankia* sp strain CpI1. J Bacteriol **172:** 1380–1384

Sellstedt A, Atkins CA (1991) Composition of amino acid compounds transported in xylem of *Casuarina* sp. J Exp Bot **42:** 1493–1498

Silvester WB, Langenstein B, Berg RH (1999) Do mitochondria provide the oxygen diffusion barrier in root nodules of *Coriaria* and *Datisca?* Can J Bot **77:** 1358–1366

Soltis DE, Soltis PS, Chase MW, Mort ME, Albach DC, Zanis M, Savlainen V, Hahn WH, Hoot SB, Fay MF, et al (2000) Angiosperm phylogeny inferred from a combined data set of 18S rDNA, *rbcL,* and *atpB* sequences. Bot J Linn Soc **133:** 381–461

Stanford AC, Larsen K, Barker GD, Cullimore JV (1993) Differential expression within the glutamine synthetase gene family of the model legume *Medicago truncatula.* Plant Physiol **103:** 73–81

Sukanya R, Li M-G, Snustad DP (1994) Root- and shoot-specific responses of individual glutamine synthetase genes of maize to nitrate and ammonium. Plant Mol Biol **26:** 1935–1946

Swensen SM (1996) The evolution of actinorhizal symbioses: evidence for multiple origins of the symbiotic association. Am J Bot **83:** 1503–1512

Swofford D (1998) PAUP*: Phylogenetic Analysis Using Parsimony (*and Other Methods). Sinauer Associates, Sunderland, MA

Temple SJ, Heard J, Ganter G, Dunn K, Sengupta-Gopalan C (1995) Characterization of a nodule-enhanced glutamine synthetase from alfalfa: nucleotide sequence, *in situ* localization, and transcript analysis. Mol Plant Microbe Interact **8:** 218–227

Thompson JD, Higgins DG, Gibson TB (1994) ClustalW: improving the sensitivity of progressive multiple alignment through sequence weighting, position specific gap penalties, and weight matrix choice. Nucleic Acids Res **22:** 4673–4680

Tingey SV, Coruzzi GM (1987) Glutamine synthetase of *Nicotiana plumbaginifolia*: cloning and in vivo expression. Plant Physiol **84:** 366–373

Tingey SV, Tsai FY, Edwards JW, Walker EL, Coruzzi GM (1988) Chloroplast and cytosolic glutamine synthetase are encoded by homologous nuclear genes which are differentially expressed in vivo. J Biol Chem **263:** 9651–9657

Tingey SV, Walker EL, Coruzzi GM (1987) Glutamine synthetase genes of pea encode distinct polypeptides which are differentially expressed in leaves, roots and nodules. EMBO J **6:** 1–9

Tjepkema JD, Schwintzer CR, Monz CA (1988) Time course of acetylene reduction in nodules of five actinorhizal plants. Plant Physiol **86:** 581–583

van de Wiel C, Scheres B, Franssen H, van Lierop MJ, van Lammeren A, van Kammen A, Bisseling T (1990) The early nodulin transcript *ENOD2* is located in the nodule parenchyma (inner cortex) of pea and soybean root nodules. EMBO J **9:** 1–7

Watanabe A, Hamada K, Yokoi H, Watanabe A (1994) Biphasic and differential expression of cytosolic glutamine synthetase genes of radish during seed germination and senescence of cotyledons. Plant Mol Biol **26:** 1807–1817

Waters JK, Hughes BL, Purcell LC, Gerhardt KO, Mawhinney TP, Emerich DW (1998) Alanine, not ammonia, is excreted from N_2-fixing soybean nodule bacteroids. Proc Natl Acad Sci USA **95:** 12038–12042

Wheeler CT, Bond G (1970) The amino acids of non-legume root nodules. Phytochemistry **9:** 705–708

Woodall J, Boxall JH, Forde BG, Pearson J (1996) Changing perspectives in plant nitrogen metabolism: the central role of glutamine synthetase. Sci Prog **79:** 1–26